Cell Reports, Volume *30*

Supplemental Information

Ultrastructural Correlates of Presynaptic Functional Heterogeneity in Hippocampal Synapses

Lydia Maus, ChoongKu Lee, Bekir Altas, Sinem M. Sertel, Kirsten Weyand, Silvio O. Rizzoli, JeongSeop Rhee, Nils Brose, Cordelia Imig, and Benjamin H. Cooper

Figure S1

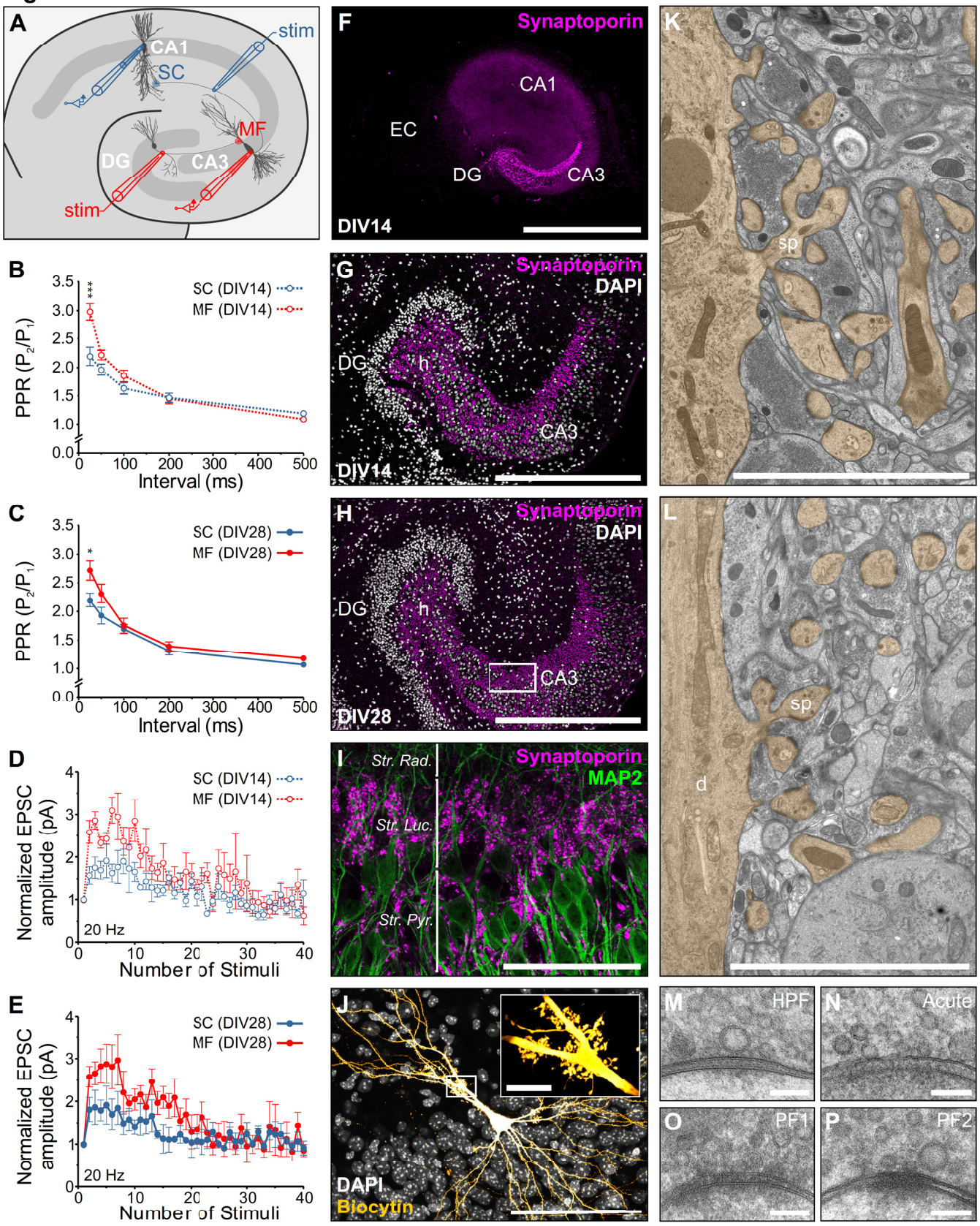
A
CA1
SC
stim
MF
DG
CA3
stim
B
PPR (P2/P1)
SC (DIV14)
MF (DIV14)
***
Interval (ms)
C
PPR (P2/P1)
SC (DIV28)
MF (DIV28)
*
Interval (ms)
D
Normalized EPSC amplitude (pA)
SC (DIV14)
MF (DIV14)
20 Hz
Number of Stimuli
E
Normalized EPSC amplitude (pA)
SC (DIV28)
MF (DIV28)
20 Hz
Number of Stimuli
F
Synaptoporin
CA1
EC
DG
CA3
DIV14
G
Synaptoporin
DAPI
DG
h
CA3
DIV14
H
Synaptoporin
DAPI
DG
h
CA3
DIV28
I
Str. Rad.
Str. Luc.
Str. Pyr.
Synaptoporin
MAP2
J
DAPI
Biocytin
K
sp
L
sp
d
M
HPF
N
Acute
O
PF1
P
PF2

Figure S1: Related to Figure 1. Functional and Morphological Characterization of the MF-CA3 Synapse.

(**A**) Schematic illustrating the experimental configurations used to characterize Schaffer collateral (blue) and MF (red) synapse transmitter release properties in organotypic hippocampal slices.

(**B**, **C**) The paired pulse ratio (PPR) measured at Schaffer collateral (SC) and MF synapses at DIV14 (**B**) and DIV28 (**C**).

(**D**, **E**) Normalized EPSC amplitudes evoked by delivery of 20 Hz action potential trains at DIV14 (**D**) and DIV28 (**E**).

(**F**-**H**) Immunoreactivity for the MF-enriched synaptic vesicle protein Synaptoporin (magenta) is restricted to the hilus and CA3 *stratum lucidum* at DIV14 (**F**, **G**) and DIV28 (**H**), indicating that target specificity of the MF-CA3 projection remains intact during this developmental period in cultured slices.

(**I**) Synaptoporin-positive MF boutons (magenta) contact MAP2-immunoreactive primary dendrites of CA3 pyramidal cells (green) within the *stratum lucidum*.

(**J**) Complex, multi-compartmental spines (thorny excrescences) forming the characteristic postsynaptic target of the MF-CA3 axon projection decorate the primary apical dendrite of a biocytin-filled CA3 pyramidal cell ('orange hot' lookup table) in a cultured hippocampal slice (insert, enlarged view of complex spines framed by white box).

(**K**, **L**) Electron micrograph of the *stratum lucidum* from a HPF cultured slice (**E**) and a perfusion-fixed hippocampus (**F**) [postsynaptic elements including dendrites (d) and spines in orange].

(**M-P**) Electron micrographs of MF-CA3 spine synapses from a cultured hippocampal slice prepared by HPF (DIV28; **M**), from an acute brain slice prepared at postnatal day (P)18 by HPF (**N**), and from perfusion fixed tissue (P28) with either 4% PFA, 2.5% GA in 0.1M PB (PF1; **O**) or 2% PFA, 2.5% GA in 0.1 cacodylate buffer (PF2; **P**).

Abbreviations: EC, entorhinal cortex; DG, dentate gyrus; CA1/3, *Cornu Ammonis* 1 and 3; Str. Rad., *Stratum Radiatum*; Luc., *Lucidum*; Pyr., *Pyramidale*; d, dendrite; sp, spine.

Scale bars: **F**, 1µm; **G**, **H**, 500 µm; **I**, **J**, 100 µm; **Insert in J**, 10 µm; **K**, **L**, 5 µm; **M**-**P**, 100 nm. Values indicate mean ± SEM; *p<0.05; **p<0.01; ***p<0.001.

Figure S2

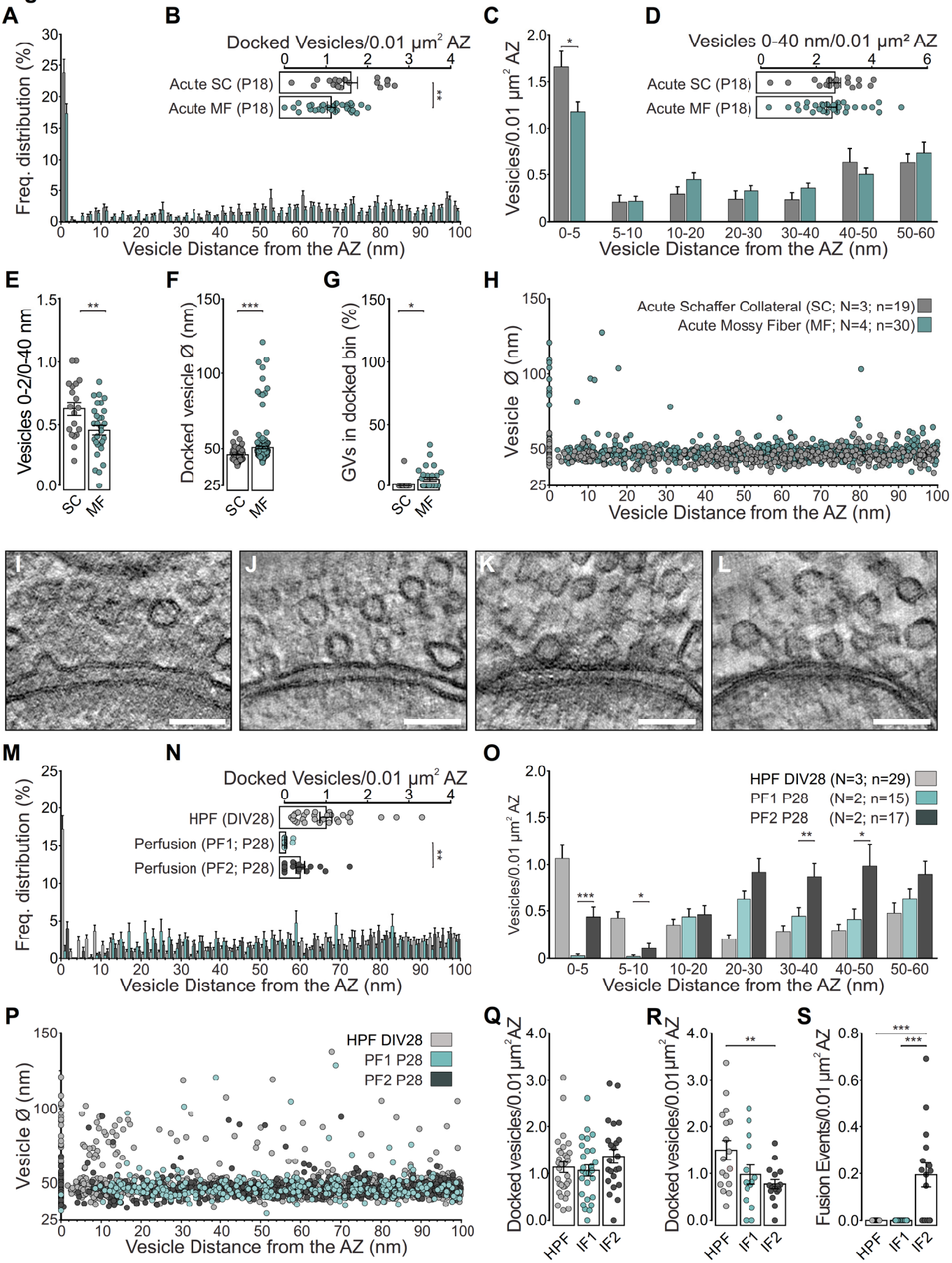
A
B
C
D
Freq. distribution (%)
Vesicle Distance from the AZ (nm)
Docked Vesicles/0.01 µm² AZ
Acute SC (P18)
Acute MF (P18)
Vesicles/0.01 µm² AZ
Vesicles 0-40 nm/0.01 µm² AZ
0-5
5-10
10-20
20-30
30-40
40-50
50-60
E
F
G
H
Vesicles 0-2/0-40 nm
Docked vesicle Ø (nm)
GVs in docked bin (%)
SC
MF
Vesicle Ø (nm)
Acute Schaffer Collateral (SC; N=3; n=19)
Acute Mossy Fiber (MF; N=4; n=30)
I
J
K
L
M
N
O
HPF (DIV28)
Perfusion (PF1; P28)
Perfusion (PF2; P28)
HPF DIV28 (N=3; n=29)
PF1 P28 (N=2; n=15)
PF2 P28 (N=2; n=17)
P
Q
R
S
HPF DIV28
PF1 P28
PF2 P28
Docked vesicles/0.01 µm² AZ
Fusion Events/0.01 µm² AZ
HPF
IF1
IF2

Figure S2: Related to Figure 2 and Table S1. Ultrastructural Effects of Different Sample Preparation and Fixation Methods on Presynaptic SV Pools.

(**A-H**) Analysis of vesicle pools in Schaffer collateral (N = 3 mice; n =19 tomograms) and MF synapses (N = 4 mice; n = 30 tomograms) in acute brain slices prepared at P18 by HPF (frozen in 20% BSA in ACSF) immediately after dissection.

(**A**) Spatial distribution of vesicles within 100 nm of the active zone (AZ) membrane.

(**B**) Scatterplots of the mean number of docked clear-cored vesicles (SVs and giant vesicles) normalized to AZ area.

(**C**) Mean number of vesicles within bins of 5 nm and 10 nm from the AZ normalized to AZ area.

(**D**) Scatterplots of vesicles within 40 nm of the AZ membrane normalized to AZ area.

(**E**) Scatterplot of the relative proportion of docked vesicles within 40 nm of the AZ normalized to AZ area.

(**F**) Scatterplot of SV diameters for all docked vesicles analyzed (Schaffer collateral, n = 113 vesicles; MF, n = 197 vesicles).

(**G**) Scatterplot indicating the respective proportions of the docked vesicle pool occupied by giant vesicles (GV; diameter > 60 nm).

(**H**) Plot of vesicle diameters for all vesicles analyzed and their respective distance to the AZ membrane.

(**I**-**L**) Comparison of MF synaptic ultrastructure in postnatal day (P) 28 WT mice perfused with either 4% paraformaldehyde (PFA), 2.5% glutaraldehyde (GA) in 0.1 M phosphate buffer (PF1; ET subvolume shown in **I**) or with 2% PFA, 2.5% GA, 2 mM $CaCl_2$ in 0.1 M cacodylate buffer (PF2; ET subvolume shown in **L**) and of organotypic slices at DIV28 immersion fixed with either 4% paraformaldehyde (PFA), 2.5% glutaraldehyde (GA) in 0.1 M phosphate buffer (IF1; ET subvolume shown in **M**) or with 2% PFA, 2.5% GA, 2 mM $CaCl_2$ in 0.1 M cacodylate buffer (IF2; ET subvolume shown in **N**) or cryo-fixed at DIV28.

(**M**) Spatial distribution of vesicles within 100 nm of the AZ membrane in perfusion-fixed material from P28 WT mice (N = 2 mice; Fixative 1 n = 15 tomograms; Fixative 2 n = 17) and WT slice cultures cryo- fixed at DIV28 (N = 3 cultures; n = 28).

(**N**) Scatterplot of the mean number of docked clear-cored vesicles (SVs and giant vesicles) normalized to AZ area in MF synapses from perfused brains and age-matched slice cultures prepared by high-pressure freezing cryofixation.

(**O**) Mean number of vesicles within bins of 5 nm and 10 nm from the AZ normalized to AZ area.

(**P**) Plot of vesicle diameters for all vesicles analyzed and their respective distance to the AZ membrane.

(**Q**) Scatterplot of the mean number of docked clear-cored vesicles (SVs and giant vesicles) normalized to AZ area in mossy fibers from age-matched aldehyde immersed and cryofixed slice cultures at approximately 5 µm from the slice surface.
(**R**) Scatterplot of the mean number of docked clear-cored vesicles (SVs and giant vesicles) normalized to AZ area in mossy fibers from age-matched aldehyde immersed and cryofixed slice cultures at approximately 20 µm from the slice surface.
(**S**) Scatterplot of the number of morphological exocytotic fusion events per tomogram normalized to AZ area at approximately 20 µm from the slice surface.
Scale bars: **I**-**L**, 100 nm. Values indicate mean ± SEM; *p<0.05; **p<0.01; ***p<0.001.

Figure S3

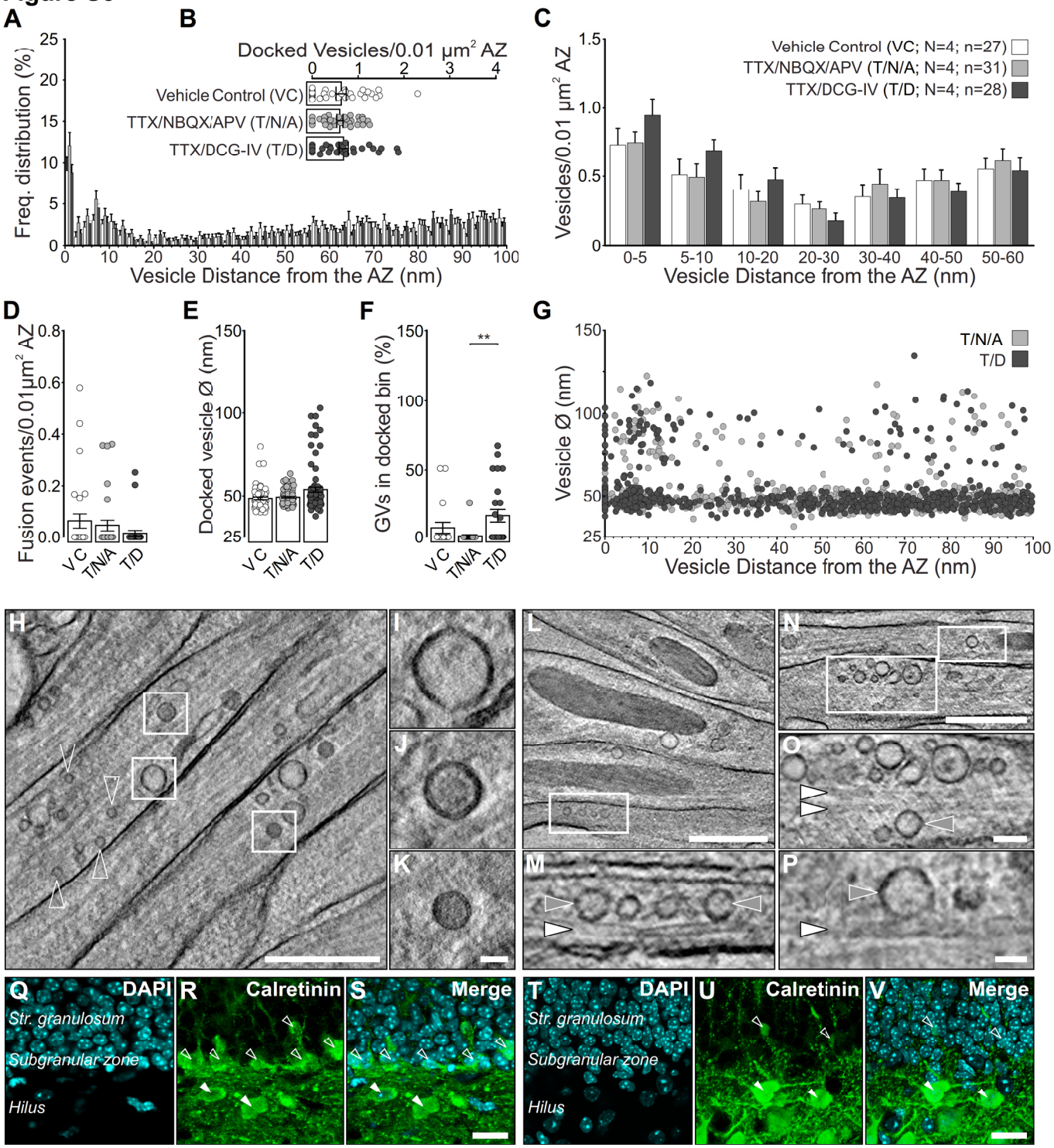
A
B
Docked Vesicles/0.01 µm² AZ
Vehicle Control (VC)
TTX/NBQX/APV (T/N/A)
TTX/DCG-IV (T/D)
Freq. distribution (%)
Vesicle Distance from the AZ (nm)
C
Vehicle Control (VC; N=4; n=27)
TTX/NBQX/APV (T/N/A; N=4; n=31)
TTX/DCG-IV (T/D; N=4; n=28)
Vesides/0.01 µm² AZ
0-5
5-10
10-20
20-30
30-40
40-50
50-60
Vesicle Distance from the AZ (nm)
D
Fusion events/0.01µm² AZ
E
Docked vesicle Ø (nm)
F
GVs in docked bin (%)
**
V C
T/N/A
T/D
G
T/N/A
T/D
Vesicle Ø (nm)
Vesicle Distance from the AZ (nm)
H
I
J
K
L
N
O
M
P
Q
DAPI
Str. granulosum
Subgranular zone
Hilus
R
Calretinin
S
Merge
T
DAPI
U
Calretinin
V
Merge

Figure S3: Related to Figure 3 and Table S1. Investigating the Origin of Giant Vesicles in MF boutons,

(**A**-**G**) Characterization of vesicle pools in MF synapses (N = 4 cultures) treated for 10 min with either vehicle control (VC; slice culture medium; n = 27 tomograms), 1 μM TTX, 2 μM NBQX, and 50 μm APV (T/N/A; n = 31), or 1 μM TTX and 2 μM DCG-IV (T/D; n = 28).

(**A**) Spatial distribution of vesicles within 100 nm of the AZ membrane in MF synapses.

(**B**) Scatterplot of docked vesicles normalized to AZ area.

(**C**) Mean number of vesicles within bins of 5 and 10 nm from the AZ normalized to AZ area.

(**D**) Scatterplot of the number of morphological exocytotic fusion events per tomogram normalized to AZ area.

(**E**) Scatterplot of vesicle diameters for all docked vesicles analyzed (VC = 62; T/N/A = 72; T/D = 83 vesicles).

(**F**) Scatterplot indicating the respective proportions of docked vesicle pools occupied by giant vesicles (GV; diameter > 60 nm).

(**G**) Plot of vesicle diameters for all vesicles analyzed and their respective distance to the AZ membrane.

(**H**-**P**) Morphological characterization of vesicle pools in MF axon bundles in the *stratum lucidum* of P18 acute hippocampal slices.

(**H**, **L**, and **N**) Tomographic subvolume (42 nm-thick) through MF axon bundles. White boxes indicate regions enlarged in I-K, M, O, and P.

(**H**-**K**) Mossy fiber axons contain multiple vesicle classes, including small clear-cored vesicles (open arrowheads in **H**), large clear-cored vesicles (**I**), and DCVs (**J** and **K**)

(**L**, **N**, and **O**) Single tomographic slices (2.8 nm-thick) reveal close contact between large clear-cored vesicles (grey arrowheads; **L**, Ø=60 and 64 nm; **N**, Ø=87 nm; **O**, Ø=81 nm) and microtubules (white arrowheads), indicative of active axonal transport between granule cell bodies and MF boutons.

(**Q**-**V**) Characterization of neurogenesis in the hippocampus of P28 mice (**Q**-**S**) and cultured hippocampal slices at DIV28 (**T**-**V**). Adult mice exhibit calretinin-positive (green) immature granule cells (open arrow head) in the subgranular zone of the dentate gyrus (cell bodies in cyan labeled by DAPI) and hilar Mossy cells (white arrowhead). In cultured hippocampal slices, calretinin-immunoreactivity is almost exclusively restricted to hilar Mossy cells, indicating an almost complete loss of immature granule cells in the DG.

Scale bars: **H**, **L**, and **N**, 500 nm; **O**, 100 nm; **I**-**K**, **M**, **P**, 50 nm; **S**, **V**, 20 μm. Values indicate mean ± SEM; *p<0.05; **p<0.01; ***p<0.001.